

Platelet rich plasma-complexed hydrogel glue enhances skin wound healing in a diabetic rat model

YUNLONG ZHANG^{1,#}; JINGWEI ZHANG^{2,#}; YU ZHU¹; BIN CAI^{1,*}

¹ Department of Orthopedic Surgery, Shanghai Jiao Tong University Affiliated Sixth People's Hospital, Shanghai, 200233, China

² Department of Orthopedics, Shanghai Fengxian District Central Hospital/Southern Medical University Affiliated Fengxian Hospital, Shanghai, 201400, China

Key words: Platelet-rich plasma, Wound healing, Umbilical cord blood, Hydrogel glue, Angiogenesis

Abstract: Diabetic patients often exhibit delayed or incomplete progress in the healing of acute wounds, owing to poor blood perfusion. Platelet-rich plasma (PRP) has attracted much attention as a means to improve wound healing, because it contains high growth factor concentrations. However, the burst-like release of PRP growth factors results in a short half-life of these therapeutic proteins, thus greatly limiting the therapeutic effect. In this study, we prepared PRP from human umbilical cord blood and developed an *in situ* photocrosslinkable PRP hydrogel glue (HNPRP) by adding a photoresponsive hyaluronic acid (HA-NB) into PRP. The HNPRP hydrogel allowed for controlled release of platelet-derived growth factor-BB (PDGF-BB) and transforming growth factor- β (TGF- β) for up to 28 days. *In vitro* cell culture showed that HNPRP promoted migration of fibroblasts and keratinocytes as well as PRP and did not reveal the advantages of HNPRP. However, in a diabetic rat skin wound model, HNPRP treatment promoted faster wound closure. Furthermore, the HNPRP group, compared with the control, PRP and hydrogel only groups, showed significantly greater re-epithelialization and numbers of both newly formed and mature blood vessels. The HNPRP group also displayed higher collagen formation than did the control group. In conclusion, HNPRP enhances angiogenesis and skin regeneration and consequently achieves faster wound healing, thus extending its potential for clinical applications to treat diabetic skin wounds.

Introduction

Wound healing, a normal biological process that restores tissue homeostasis in the human body, requires the activation of platelets and a cascade of released factors. Patients with diabetes often exhibit impaired healing of acute wounds because of deficient blood flow, thus increasing the complications and risks during treatment (Natarajan *et al.*, 2000; Steed *et al.*, 2006). Hence, there is an urgent need to explore effective treatments for wound healing in diabetes (Fehse *et al.*, 2001).

Platelet-rich plasma (PRP) and fibrin-based biomaterials, known as fibrin glues or fibrin sealants, have been used for more than 30 years and have demonstrated benefits in almost all surgical fields, including reconstructive plastic surgery and wound treatment (Burnouf *et al.*, 2013). The activation of platelets and the release of growth factors are the key aspects of natural wound repair and tissue

regeneration (Borrione *et al.*, 2010; Gelmini *et al.*, 2001; Nakanishi *et al.*, 2001). PRP derived from human umbilical cord blood (HUCB) rather than peripheral blood has a higher content of growth factors, such as platelet derived growth factor (PDGF), transforming growth factor- β (TGF- β), fibroblast growth factor, epidermal growth factor and vascular endothelial growth factor (Andrade *et al.*, 2020; Murphy *et al.*, 2012). Moreover, the application of the allogeneic HUCB-PRP may circumvent the practical limitations preventing the clinical use of autologous platelet gel in groups of patients such as elderly hypo-mobile patients, neonates and children for whom repeated blood collections for multiple PRP gel applications might be difficult or clinically inappropriate (Rebulla *et al.*, 2016), and clinical study has shown that allograft PRP injection is safe in the treatment of rotator cuff disease (Jo *et al.*, 2020).

Several challenges remain in the application of PRP for management of clinical wounds. First, the use of bovine thrombin is associated with a risk of inducing immunological reactions characterized by the generation of cross-reactive anti-human factor V or anti-thrombin antibodies (Clark *et al.*, 2008). The rapid activation of platelets and the cascade

*Address correspondence to: Bin Cai, 7250012860@shsmu.edu.cn

#These two authors contributed equally to this study

Received: 30 December 2020; Accepted: 13 May 2021



of released factors lead to short lifetimes of the growth factors present or their early inactivation and degradation by numerous hydrolytic enzymes at the wound site (La and Yang, 2015). Moreover, activation by thrombin immediately before implantation significantly inhibits the activity of PRP (Han et al., 2009). Therefore, a suitable scaffold with the ability to provide controlled release of many growth factors is needed for topical application of PRP during wound healing. Among various biomaterials, hydrogels that share many properties with soft tissue have become a research hotspot (Xue et al., 2019). Many types of hydrogels have been researched in dermal wound healing, such as bisphosphonate-functionalized hydrogel (Guven et al., 2018), chitosan hydrogel (Ponsubha and Jaiswal, 2020) and thermoresponsive hydrogel (Zhu et al., 2016). However, none of these materials allow for stable biological fixation, which is crucial in constructing the wound barrier and maintaining the applied agent (Dreifke et al., 2015). An ideal integration requires a close, preferably chemically bonded, interface between the hydrogel and tissue surface (Gristina, 1987). Herein, we designed a novel PRP-complexed hydrogel (HNPRP) capable of *in situ* gelatinization and tight integration with wounds through a phototriggered-imine-crosslinking reaction, which not only solved the problem that PRP was not suitable for adhesion in the past, but also effectively carried out the slow release of growth factors in PRP.

In the present work, double centrifugal method was used to extract PRP, which could effectively remove almost all cellular components in umbilical cord blood and avoid rejection reaction. And we first successfully prepared HUCB-PRP-complexed hydrogel, then evaluated its application in wound healing at the cellular level and in an STZ-induced diabetic rat skin wound model. We hypothesized that this new gel loaded with a certain concentration of PRP derived from HUCB might effectively promote tissue repair during wound healing.

Materials and Methods

Preparation of the HNPRP hydrogel

Human cord blood samples were collected from healthy parturients during delivery. Fresh plasma was obtained within 6 h of collection from the parturients to maintain the bioactivity of cytokines and growth factors. The plasma was centrifuged at 200 *g* for 15 min, then the plasma together with the platelets were re-centrifuged at 150 *g* for 10 min. Finally, PRP was isolated by discarding the red blood cell fraction at the bottom. The PRP was activated in the form of a gel by using 10 U/mL bovine thrombin (Sigma-Aldrich, St. Louis, MO, USA) and 2.5 mM CaCl₂. For all experiments in this study, PRP was standardized to a concentration of 10⁶ platelets/mL by dilution with sterile saline solution. Concentrated PRP was stored at -80°C until use to preserve its function. This study was approved by the Ethics Committee of the Sixth People's Hospital of Shanghai Jiao Tong University. HUCB samples were collected after written informed consent was obtained from all participants.

Photoresponsive hyaluronic acid (HA-NB) generated aldehyde groups under light irradiation, which subsequently reacted with amino groups in the PRP components, such as

fibrinogen. HA-NB was synthesized according to a previous report (Yang et al., 2016). The graft content of nitrobenzene (NB) in hyaluronic acid was approximately 6%. To prepare HNPRP hydrogel, HA-NB was fully dissolved in the obtained PRP solution at a concentration of 3% w/v. Then a 395 nm-LED (20 mW/cm², 1 min) was used to prepare the HNPRP hydrogel. The platelet concentration in PRP was determined by double centrifugation method. The platelet concentration in PRP was adjusted to 1 × 10⁶ units/μL by sterilized PBS. The platelet concentration in PRP was used as standard PRP for *in vitro* and *in vivo* experiments.

Characterization of the HNPRP hydrogel

The dynamic rheological properties of the HNPRP hydrogel under light irradiation was detected with a HAAKE MARS III (Thermo Scientific, Karlsruhe, Germany) rheometer equipped with an OmniCure S2000 lamp (320–500 nm, light intensity of 395 nm: 40 mW/cm²). 200 μL HNPRP hydrogel precursor solution was added to the rheometer. Then the storage modulus (*G'*) and loss modulus (*G''*) were recorded with increasing irradiation time at a frequency of 1 Hz and γ of 10%.

The morphology of freeze-dried HNPRP hydrogel was observed by scanning electron microscopy (SEM). HNPRP hydrogel (50 μL) was prepared and freeze-dried for 24 h. The freeze-dried sample was coated with gold and observed by SEM at 15.0 kV.

The swelling properties of HNPRP hydrogel were evaluated by immersion in phosphate buffered saline (PBS, pH = 7.4), which the pH accomplished the requirements for diabetic wound injuries (Mcardle et al., 2014). Briefly, six pieces of 100 μL HNPRP hydrogel disks with a diameter of 5 mm were precisely weighed, and the initial weight was recorded as *W*₀. The hydrogel disks were then immersed in PBS at 37°C. Then, at specific time points (1, 2, 4, 8, 16, and 24 h after immersion in saline); the samples were removed from the tubes and gently blotted with filter paper to remove excess water on the surface. The mass of each sample was recorded as *W*_{*t*}. The swelling ratio at each time point was calculated as *W*_{*t*}/*W*₀.

Release kinetics of growth factors

The release of PDGF-BB and TGF-β from PRP gel and HNPRP hydrogel *in vitro* was determined through enzyme-linked immunosorbent assay (ELISA) during a time course of 28 days. Briefly, 200 μL PRP gel or HNPRP hydrogel was added to a 48-well plate, and the same volume of phosphate-buffered saline (PBS) was then added. At predetermined time points, the supernatant was collected by centrifugation at 1000 *g* for 5 min and replaced with the same volume of fresh PBS. The released PDGF-BB and TGF-β were determined by measuring the concentrations in the supernatant through ELISA (R&D Systems, Minneapolis, MN, USA) according to the manufacturer's instructions.

Cell lines

Both primary fibroblasts (from mouse tail skin) and human epidermal cell line HaCaT were provided by Dr. Dawei Li, School of Pharmacy, Shanghai Jiao Tong University. Cells were cultured in Dulbecco's modified Eagle's medium

(DMEM) containing 10% fetal bovine serum (FBS), and maintained in 5% CO₂ at 37°C.

Cell migration

The effects of HNPRP on the mobility of fibroblasts and HaCaT cells was assessed through scratch wound assays, as described previously (Wang *et al.*, 2001). Briefly, the cells were grown to 80% confluence in six-well plates at 37°C in a 5% CO₂ incubator. A wound was created by scratching the cells with a sterile 200 µL pipette tip. The cells were then incubated with 100 µL of PRP gel, hydrogel glue only or HNPRP hydrogel for 12 or 24 h. Cell migration into the wound surface was determined under an inverted microscope (LSM 510, Carl Zeiss, Oberkochen, Germany). Cells that migrated across the black lines were counted in five random fields in triplicate experiments.

Diabetic rat skin wound model and treatments

All procedures were approved by the Animal Research Committee of the Sixth People's Hospital at Shanghai Jiao Tong University. Adult male Sprague–Dawley rats weighing 200–250 g were obtained from the Experimental Animal Center of Shanghai Jiao Tong University. All rats were housed in a facility with a 12 h light/dark cycle (lights out between 18:00 h and 06:00 h) at a controlled temperature (22 ± 3°C) and humidity (50 ± 15%) and were given free access to a standard diet and tap water. A type I diabetes rat model was created as previously described (Luippold *et al.*, 2012). Briefly, rats were pre-treated with a single intraperitoneal injection of 60 mg/kg STZ (Sigma–Aldrich, St. Louis, MO, USA) to induce experimental diabetes. The serum blood glucose levels were measured daily with a blood glucose meter. Animals with fed glucose levels above 16.67 mmol/L were selected and used in the different studies.

To create a skin wound model under the diabetic condition, the dorsal skin was shaved after each rat was placed under anesthesia through intraperitoneal injection of 50 mg/kg pentobarbital. Four full-thickness excisional wounds (18 mm in diameter) were created on the dorsal skin. The four wounds were randomly assigned to four different treatments, each applied to one wound: (1) 200 µL saline (control, N = 20), (2) 200 µL hydrogel alone (HG, N = 20), (3) 200 µL free PRP (PRP, N = 20) (4) or 200 µL equal PRP loading hydrogel (HNPRP, 3% w/v, N = 20). Each wound received 395 nm light irradiation for 3 min on the surface of the wound. After irradiation, Tegaderm (3M, London, ON, Canada) was placed over the wounds for protection.

Wound closure analysis

Digital photographs of wounds were taken at day 0, 7, 14, 21 in anesthetized rats placed against a ruler. Photographs were calculated with an image analysis program (NIH Image, USA). The percentage wound closure was calculated with the equation: wound closure (%) = $(A_0 - A_t)/A_0 \times 100\%$, where A_0 is the initial wound area on day 0, and A_t is the wound area at each time point post-wounding. The investigators measuring samples were blinded to group and treatment.

Six wounds per group were harvested at days 14 and 21 post-wounding, fixed with 10% buffered formalin

(Sigma–Aldrich) for 1 day and embedded in paraffin for subsequent histological and immunostaining evaluation.

Histological analysis

The paraffin-embedded samples were sectioned into 4 µm sections. The sections were stained with hematoxylin and eosin (H&E) and used to assess gross morphology and qualitative wound healing parameters such as the thickness of granulation tissue and the formation of normal dermal substructures. To examine the collagen composition, we also performed Masson's trichrome staining (Laufer *et al.*, 1974), examined samples through light microscopy (Olympus BX 45, Olympus, Hamburg, Germany), and measured collagen areas in ImagePro software (Media Cybernetics, Silver Spring, MD).

Immunofluorescence analysis

For immunofluorescence staining, dorsal skin samples from the wound sites were fixed in 4% paraformaldehyde overnight. rabbit anti-CD31 (1:100 dilution, US Abcam, Cambridge, MA) and mouse anti- α -SMA (1:50 dilution, Abcam, Cambridge, MA, USA) were used to confirm angiogenesis during the wound healing process. Alexa-Fluor 594-conjugated goat anti-rabbit and Alexa-Fluor 488-conjugated goat anti-mouse antibodies (1:200) were used as secondary antibodies, and the nuclei were counterstained with DAPI. All images were acquired with fluorescence microscopy (Olympus FluoView™ FV1000, Tokyo, Japan). The newly formed vessels were indicated by CD31 positive staining, and mature vessels were detected as CD31 and α -SMA double-positive vascular structures. Five randomly selected microscopic fields were analyzed per slide in a blinded manner, and the number of newly formed vessels and mature vessels was recorded.

Re-epithelialization was measured in day 7 wound sections stained with a rabbit antibody to polyclonal cytokeratin (1:100 dilution, Abcam). Re-epithelialization was defined as the percentage of the initial wound produced at surgery, which was calculated as: re-epithelialization (%) = $(1 - \text{distance between epithelial tongues}/\text{length of wound}) \times 100\%$ (Choi *et al.*, 2016).

Statistical analysis

The quantitative data are expressed as mean ± standard deviation (SD). All data were statistically analyzed in SPSS 22.0 software (IBM Corporation, Armonk, NY, USA). Differences were determined with one-way ANOVA followed by Tukey's *post hoc* test. The significance threshold was set at $P < 0.05$.

Results

Characterization of HNPRP hydrogel glue

First, we investigated the dynamic rheological properties of HNPRP hydrogel under light irradiation. Both the storage modulus (G') and the loss modulus (G'') increased with increasing irradiation time at the initial stage (Fig. 1A). At 15 s, the value of G' exceeded that of G'' , thus suggesting that the gel state had formed in the system. The fast gelation of HNPRP hydrogel upon irradiation aids in its application

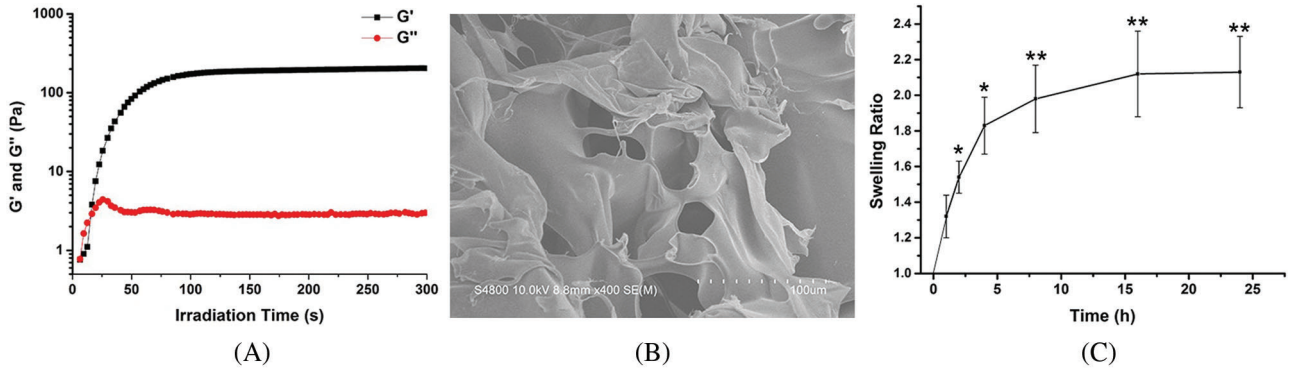


FIGURE 1. (A) Dynamic rheological properties of HNPRP hydrogel upon light irradiation. (B) SEM image of freeze-dried HNPRP hydrogel. (C) Swelling rate of HNPRP hydrogel. * $P < 0.05$, ** $P < 0.01$ compared to 1 h. The data are presented as mean \pm SD ($N = 6$).

in wound healing. At ~ 200 s, the value of G' reached ~ 200 Pa and remained stable thereafter, thus indicating the maximum storage modulus of HNPRP hydrogel. Furthermore, the HNPRP hydrogel showed a robust final storage modulus that allowed stable 3D structure to be maintained.

We then observed the morphology of freeze-dried HNPRP hydrogel. A porous 3D structure with micrometer-scale pores was observed in SEM images of freeze-dried HNPRP hydrogel (Fig. 1B). The porous structure of HNPRP hydrogel aids in nutrient transfer, growth factor delivery and cell infiltration, all of which promote tissue regeneration.

The dynamic swelling properties of the HNPRP hydrogel were investigated via saline immersion. The HNPRP hydrogel swelled rapidly within 4 h after immersion in saline (Fig. 1C, $P < 0.05$). The swelling rate then began to decline, and after 16 h, the mass of HNPRP remained constant, thus suggesting full swelling of the HNPRP hydrogel. The final swelling ratio was ~ 2.1 . Furthermore, after fully swelling, the HNPRP hydrogel maintained a stable gel structure. The swelling property of HNPRP hydrogel is important because it allows for absorption of wound exudates and maintenance of a stable structure after full swelling.

Effects of HNPRP on growth factor release kinetics

To determine whether the HNPRP hydrogel had the ability to slow the burst-like release of growth factors, ELISA was used to detect the release kinetics of PDGF-BB and TGF- β from the HNPRP hydrogel and PRP gel. The release kinetics of PDGF-BB and TGF- β indicated slower release from HNPRP than PRP. In the HNPRP hydrogel, the two factors were released progressively for 28 days, whereas in PRP gel, a clear burst-like

release was observed after 6 h for PDGF-BB and after 1 h for TGF- β ($P < 0.05$), after which the release of growth factors slowed significantly, then remained almost unchanged (Fig. 2).

Effects of HNPRP on cell migration of fibroblasts and keratinocytes

To investigate whether the HNPRP hydrogel affected the migration of fibroblasts and HaCaT cells, scratch wound assays were performed. The same trend was observed for both cell lines. Both PRP gel and HNPRP hydrogel, compared with the control, significantly promoted the migration of fibroblasts (Figs. 3A and 3B) and HaCaT cells (Figs. 3C and 3D) ($P < 0.01$ for both), and the migration rate increased with extension of the incubation time. Compared with the HaCaT cells, fibroblasts showed more active migration at 24 h in both PRP gel and HNPRP hydrogel.

Effects of HNPRP on wound healing

To assess the effects of HNPRP on wound healing, dorsal skin wounds were created in STZ-induced diabetic rats and were randomly treated with free PRP, hydrogel alone, HNPRP or saline control. Fig. 4C shows HNPRP firmly binds to the wound surface after light irradiation. Fig. 4A shows representative images of wound surfaces at days 0, 7, 14, and 21 for each group. The wound areas were significantly smaller in the HNPRP treated group than the control group on days 7, 14, and 21 ($P < 0.05$), whereas no significant differences were observed in the PRP, and hydrogel groups compared with the control group (Fig. 4B). On day 21, the wounds in the HNPRP group were almost fully healed, whereas $\sim 8\%$, 15% and 20% of the wound areas in the hydrogel group, PRP group and control group, respectively, remained open.

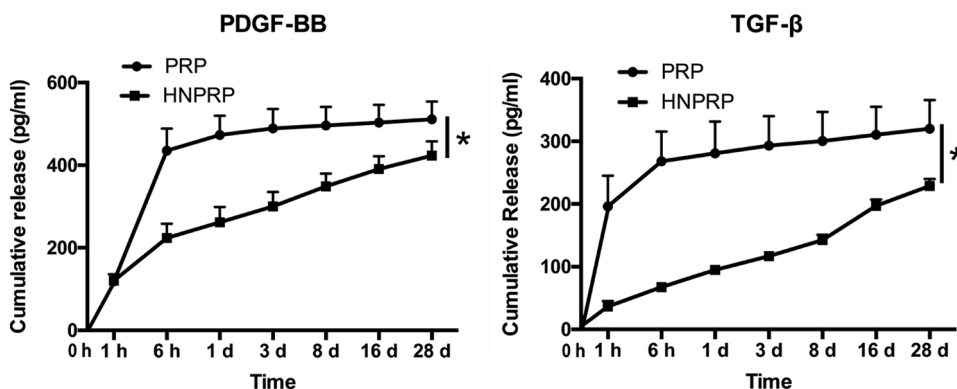


FIGURE 2. Release kinetics of PDGF-BB and TGF- β from PRP gel or HNPRP hydrogel. * $P < 0.05$. All values represent the mean \pm SD of three replicates.

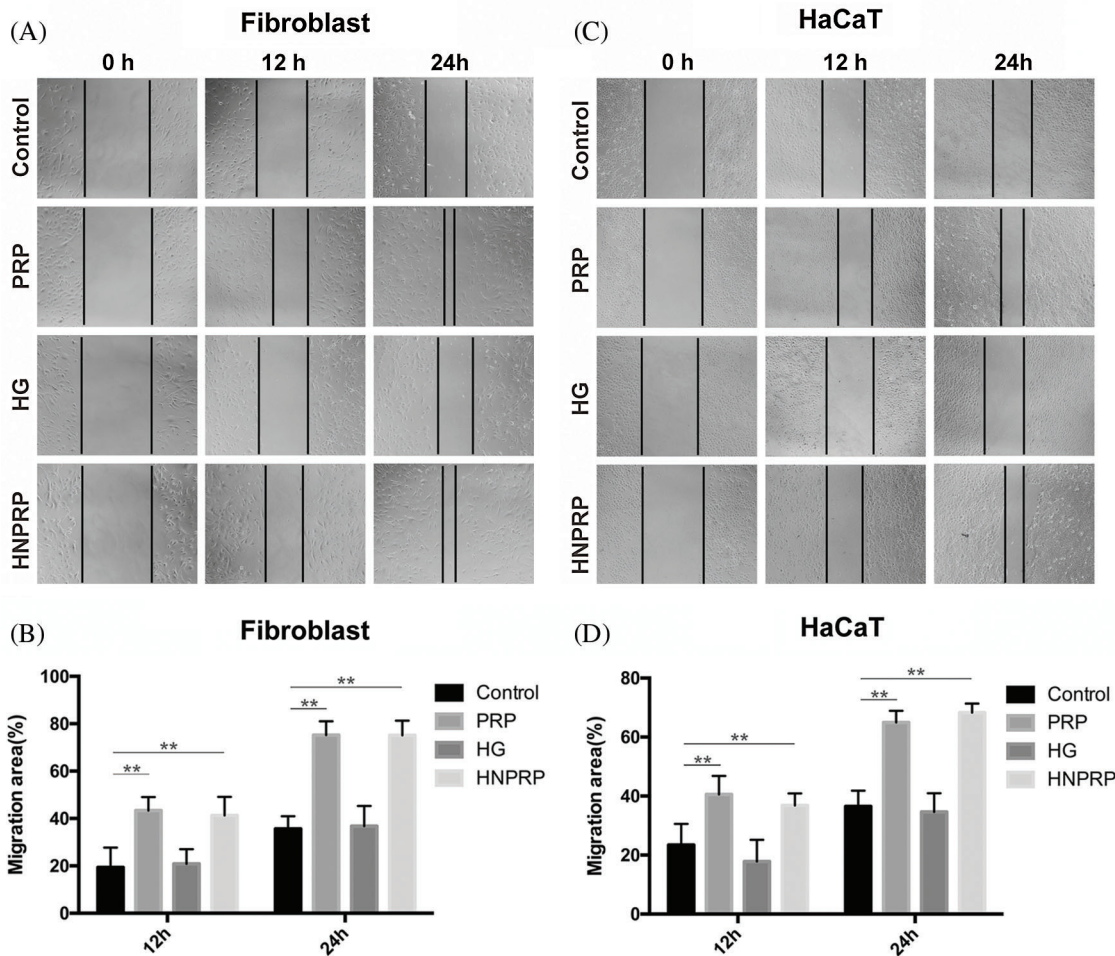


FIGURE 3. Cell migration photographs of fibroblast (A) and HaCaT (B) at different time points. (C and D) Quantification of the percentage migrated cells at 12 and 24 h. All values represent the mean ± SD of three replicates. ***P* < 0.01.

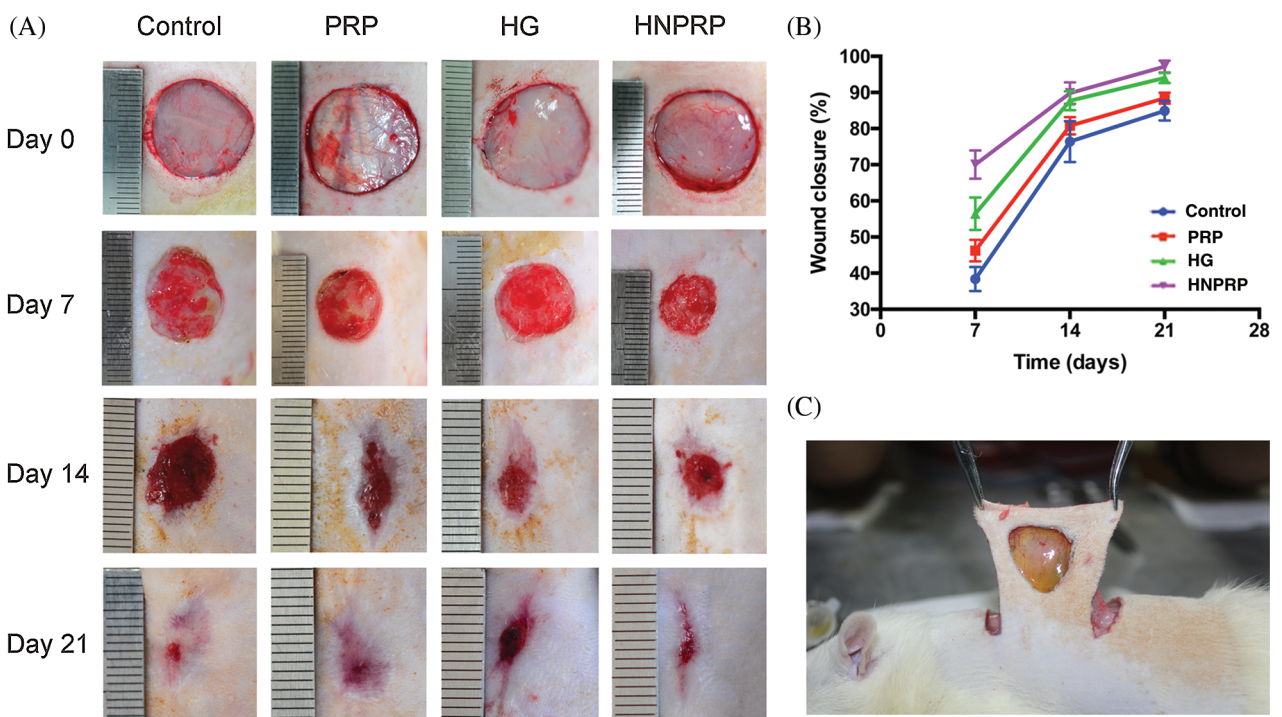


FIGURE 4. (A) Digital images of the wound area at days 0, 7, 14 and 21. (B) Quantification of the percentage wound closure. Quantitative data are shown as mean ± SD (N = 5 per time point for each group). **P* < 0.05. (C) HNPRP firmly binds to the wound surface after light irradiation.

Effects of HNPRP on re-epithelization

Histological analysis of the H&E-stained wound sections indicated that the restoration of epidermal tissues occurred faster in the HNPRP group than in the other three groups at days 14 and 21 (Fig. 5A). At days 14 and 21, wounds treated with HNPRP had significantly smaller scar widths than those of the other treated wounds, whereas the PRP and hydrogel groups showed no differences between groups (Fig. 5B, $P < 0.01$). At day 21, the HNPRP treated group showed nearly complete wound healing. We also identified epidermal cells in the wounds by immunofluorescence staining for cytokeratin (Fig. 5C). On day 7 after wounding, the HNPRP group showed significantly higher re-epithelialization than did the other groups (Fig. 5D, $P < 0.01$). The re-epithelialization in the HNPRP group was approximately 50% complete, whereas it was approximately 30% in the PRP and hydrogel groups and less than 25% in the saline group.

Effects of HNPRP on angiogenesis

To confirm the effects of HNPRP on angiogenesis during the wound healing process, immunofluorescence staining for CD31 and α -SMA was used to image newly formed and

mature blood vessels, respectively (Figs. 6A and 6B). For newly formed blood vessels, at days 14 and 21 after surgery, a significantly higher vascular density was observed in the HNPRP group compared with the other three groups, whereas there were no significant differences among the control, PRP- or HG-treated groups (Fig. 6C). At day 14, the mature blood vessel density showed the same trend as that of the newly formed blood vessels. At day 21, the HNPRP group had a significantly higher mature blood vessel density than that in the other three groups, and there was a significant difference between the HG and control groups (Fig. 6D).

Effects of HNPRP on collagen deposition

Masson's trichrome staining was used to identify collagen deposition in the wounds 14 days after surgery. Among all groups, the most collagen deposition was observed in the wounds treated with HNPRP (Fig. 7A). The HG and HNPRP groups exhibited better organized collagen deposition than did the other two groups (Fig. 7B), and the collagen areas in the HG and HNPRP groups were also significantly larger than those in the control group (Fig. 7C, $P < 0.05$).

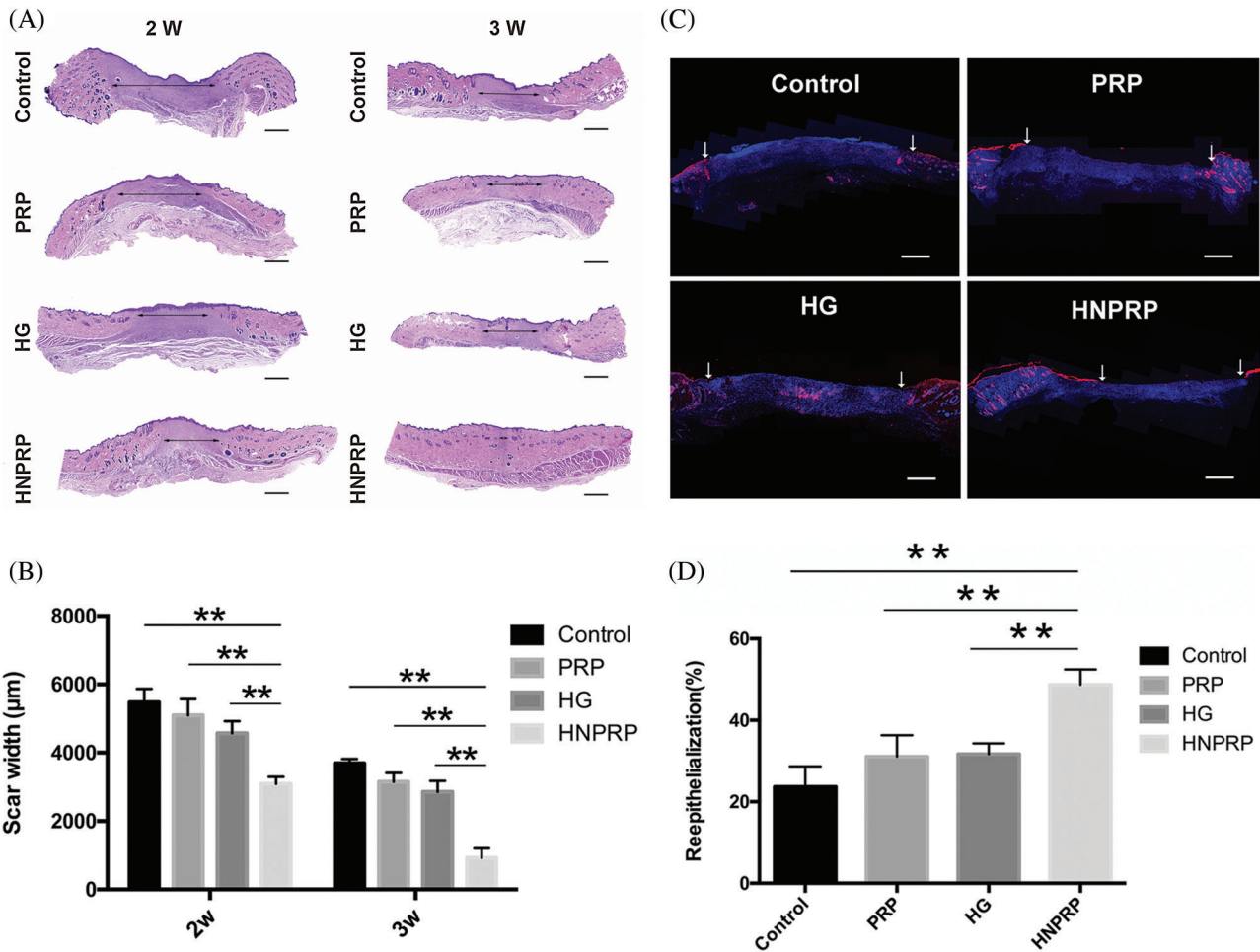


FIGURE 5. (A) Micrographs of H&E-stained tissue specimens. Arrows mark the scars. Bars = 500 µm. (B) Scar width was measured. (C) Wound sections were stained for cytokeratin and counterstained with DAPI to reveal cell nuclei. Arrows indicate the epidermal cells. Bars = 500 µm. (D) Percentage change in re-epithelialization, measured on day 7. Quantitative data are shown as mean ± SD (N = 5 per group). ** $P < 0.01$.

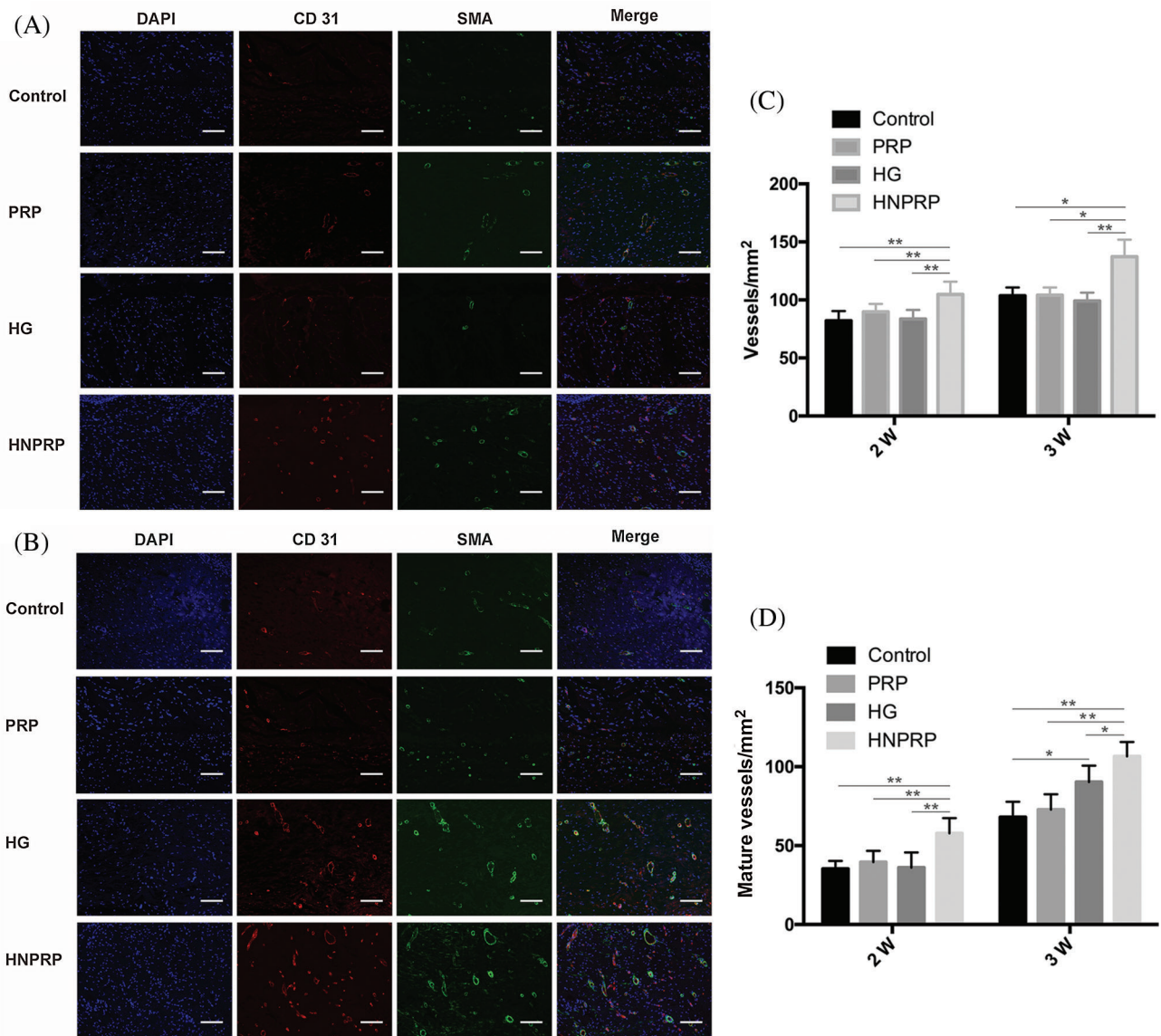


FIGURE 6. (A) immunofluorescence staining for CD31 and α -SMA on days 14 (A) and 21 (B) after wounding. Positive CD31 staining was used to reveal newly formed blood vessels. CD31 and α -SMA co-staining indicates mature blood vessels. Bars = 300 μ m. Numbers of newly formed blood vessels (C) and mature blood vessels (D) on days 14 and 21 post-surgery. Quantitative data are shown as mean \pm SD (N = 5 per group). * P < 0.05, ** P < 0.01.

Discussion

PRP contains a variety of therapeutic growth factors, the chemotactic properties of growth factors can stimulate cell proliferation and the synthesis of extracellular matrix (ECM), contributing to the repair of wound tissue that are involved in wound healing and the repair of mineralized tissue (Max *et al.*, 2001; van Elden *et al.*, 2001; Yang *et al.*, 2016). Compared with the normal wound healing process, the normal balance of the types and amounts of growth factors in the wound environment of diabetic patients is unbalanced, leading to difficulty in wound healing (Thomson *et al.*, 2010). PRP is usually used via thrombin activation to form a gel state and has wide clinical applications in fields such as orthopedics, skin surgery and sports medicine (Chen *et al.*, 2018; Jeck and Sharpless, 2014; Jessen and Mirsky, 2016; Previtali *et al.*, 2003). However, some studies have shown that the use of PRP alone does not

significantly improve conditions (Ashwal-Fluss *et al.*, 2014), and moreover the clinical utilization of PRP gel has some disadvantages. The first drawback is that the release of growth factors is temporal and has a short lifetime, thus limiting wound healing efficacy (La and Yang, 2015). Second, there is low tissue adhesiveness between the PRP gel and the wound surface, thus leading to easy loss of the gel. Third, the introduction of thrombin to activate PRP may induce an immune response during the experiment. Therefore, finding a means of slowing the release of growth factors, achieving stable tissue adhesiveness, and eliminating immune responses to PRP remain pressing problems.

HUCB has been widely used in the clinical treatment of various diseases. Compared with peripheral blood, umbilical cord blood PRP contains higher concentrations of growth factors and is not susceptible to immunological rejection (Han *et al.*, 2018; Hashemi *et al.*, 2017; Murphy *et al.*, 2012). Moreover, hydrogels have a high-water retention

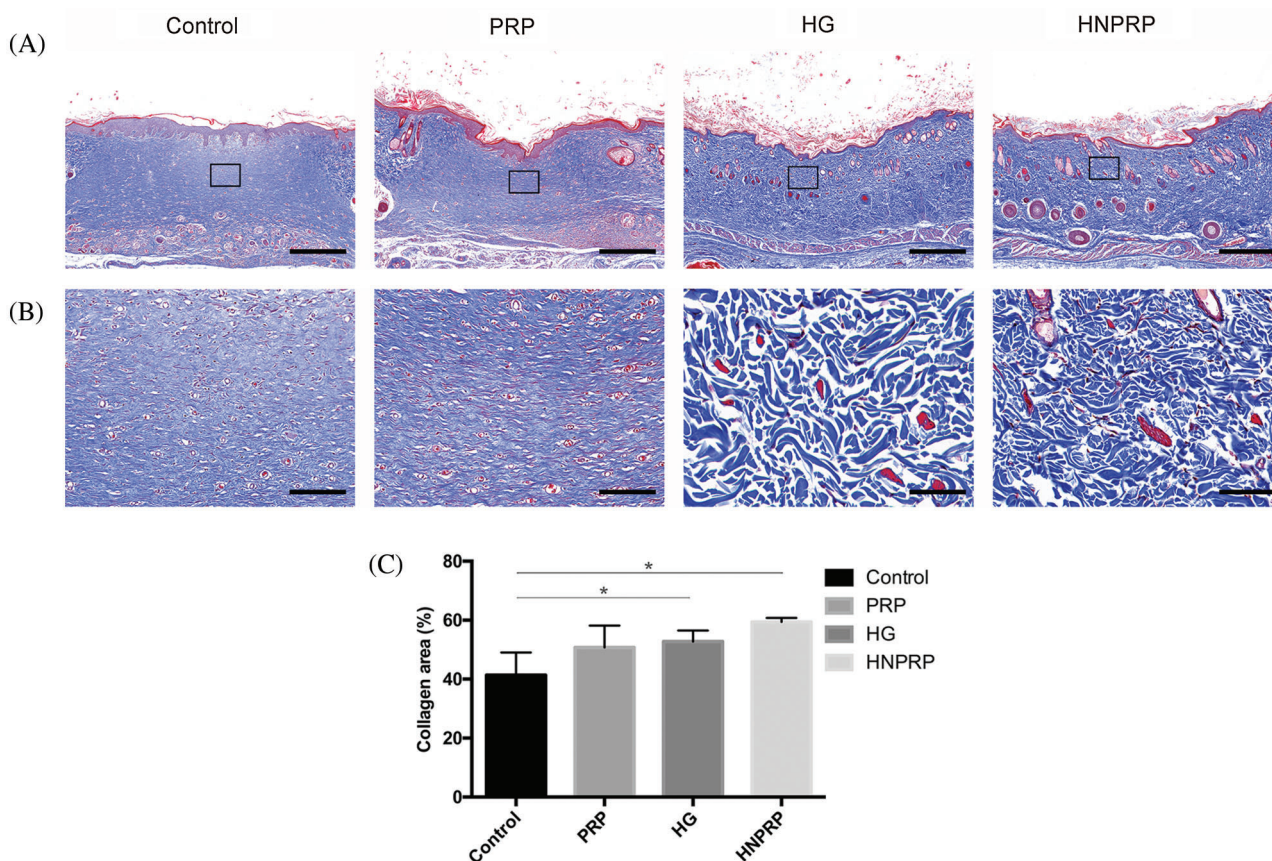


FIGURE 7. Histological analyses of wound healing at day 21, using Masson's trichrome staining, with low magnification (A, bars = 1 mm), and an enlarged view of the region inside the box of A (B, bars = 100 μ m). (C) Quantification of collagen areas. All data are shown as mean \pm SD (N = 5 per group). * $P < 0.05$.

capacity, which not only promotes the exchange of the liquid microenvironment but also prevents secretions from gathering in the wound site by promoting drainage. In our study, the HNPRP hydrogel exhibited controlled release of PDGF-BB and TGF- β for as long as 28 days, whereas free PRP exhibited only a burst-like release at 6 h for PDGF-BB and at 1 h for TGF- β . The mechanism of controlled release may be that HNPRP released a large number of growth factors, which became fixed in the hydrogel through physical interaction, and this fixation of growth factors slowed the release as the hydrogel degraded (Qiu *et al.*, 2016). Furthermore, our previous research showed that the hydrogel could perfectly fill the skin defect with strong tissue binding strength, which is of great significance in clinical applications. We believe that this characteristic of HNPRP may promote the development of therapeutic treatments for acute skin wounds.

Keratinocytes and fibroblasts play important roles in the healing process of skin wounds and can be activated by trauma. Activated cells participate in epithelialization, scar tissue formation, wound remodeling, and angiogenesis through cell proliferation and migration (Cao *et al.*, 2018; Kim *et al.*, 2017). Our *in vitro* results showed that HNPRP promoted the migration of fibroblasts and keratinocytes as well as PRP did, but it did not reflect the advantages of HNPRP. In those experiments, we used normal cells and observed no significant differences between the HNPRP and PRP groups, possibly because of that HNPRP needs to be

continuously immersed in tissue culture medium in the scratch experiment and can only play a limited role in controlled release. Wound re-epithelialization rebuilds a barrier between the wound and its surroundings, which is necessary to prevent infection (Rousselle *et al.*, 2019). Because epithelial cells can protect skin from infection, it is important in skin wound healing. In this study, we found that, compared with the control wounds, the wounds in the HNPRP treatment group healed well, and the epidermis was thicker. Keratinocytes on the wound surface moved faster than the scar tissue below in HNPRP treated wounds (Shi *et al.*, 2016). Therefore, compared with the *in vivo* experiment, the barrier protective effect of HNPRP on the wound was not demonstrated in the *in vitro* experiment, so there was no significant difference in the *in vitro* experiment, while the effect of promoting wound healing in the HNPRP group was significantly better than that in the PRP group in the *in vivo* experiment.

Fibrous tissue replacement of granulation tissue is an important biological process in wound healing (Hajimiri *et al.*, 2016). In our study, Masson's trichrome staining indicated that the greatest collagen deposition occurred in the wounds treated with HNPRP, among all groups. HNPRP promoted skin tissue remodeling, thus accelerating wound healing. The elevated blood glucose in diabetic patients can decrease protein synthesis and consequently result in cell metabolic abnormalities, which cause a decline in fibroblast function and collagen deposition at wound sites

(Saidian *et al.*, 2019). These responses can in turn cause the tensile strength of the wound to be insufficient, thus affecting wound healing.

New blood vessel formation is a key factor in wound healing, because new blood vessels can provide oxygen and nutrients, and also transport cells and secretion factors that are necessary for healing to the wound area (Michalczyk *et al.*, 2020). In addition, the growth of blood vessels is dependent on the stability of the surrounding smooth muscle cells. Newly formed blood vessels were detected on the basis of CD31 positive staining, and mature vessels were detected as CD31 and α -SMA double-positive vascular structures (Petersen *et al.*, 2018). Vascular disease in patients with diabetes can cause a deficiency in nutrient supply and hinder the repair of local wound tissue. In this study, the HNPRP group showed significantly more newly formed and mature blood vessels than were found in the control, PRP and hydrogel only groups. Thus, HNPRP was beneficial to the formation of granulation tissue and collagen, and further accelerated wound healing. However, there are still some shortcomings in our study. For example, *in vitro* study, we did not simulate the environment of diabetic wound to confirm the effect of our new material on promoting cell migration.

Conclusion

This study showed that HNPRP hydrogel can slow the burst-like release of growth factors from PRP and promote the migration of fibroblasts and keratinocytes *in vitro*. In a diabetic rat skin wound model, HNPRP can accelerate wound healing by enhancing angiogenesis and skin regeneration. Overall, HNPRP extends the potential for clinical application of hydrogels to treat diabetic skin wounds. However, because only five animals were used at each time point in this study, and only one treatment concentration was assessed at each time point, we cannot be sure whether HNPRP's curative effects exhibit dose dependency. In the future, we will optimize the HNPRP dose to achieve faster wound healing.

Availability of Data and Materials: All data generated or analyzed during this study are included in this published article.

Author Contribution: The authors confirm contribution to the paper as follows: study conception and design: YLZ, JWZ, BC; data collection: YLZ, YZ; analysis and interpretation of results: JWZ, YZ; draft manuscript preparation: YLZ, JWZ. All authors reviewed the results and approved the final version of the manuscript.

Ethics Approval: All procedures were approved by the Animal Research Committee of the Sixth People's Hospital at Shanghai Jiao Tong University. Ethical approval code: 2017-0202, Date of approval: 28 February 2017.

Funding Statement: The authors received no specific funding for this study.

Conflicts of Interest: The authors declare that they have no conflicts of interest to report regarding the present study.

References

- Andrade SS, De Sousa Faria AV, de Paulo Queluz D, Ferreira-Halder CV (2020). Platelets as a 'natural factory' for growth factor production that sustains normal (and pathological) cell biology. *Biological Chemistry* **401**: 471–476.
- Ashwal-Fluss R, Meyer M, Pamudurti NR, Ivanov A, Bartok O et al. (2014). circRNA biogenesis competes with pre-mRNA splicing. *Molecular Cell* **56**: 55–66.
- Borrione P, Gianfrancesco AD, Pereira MT, Pigozzi F (2010). Platelet-rich plasma in muscle healing. *American Journal of Physical Medicine & Rehabilitation* **89**: 854–861.
- Burnouf T, Goubran HA, Chen TM, Ou KL, El-Ekiaby M, Radosevic M (2013). Blood-derived biomaterials and platelet growth factors in regenerative medicine. *Blood Reviews* **27**: 77–89.
- Cao X, Wang Y, Wu C, Li X, Fu Z et al. (2018). Cathelicidin-OA1, a novel antioxidant peptide identified from an amphibian, accelerates skin wound healing. *Scientific Reports* **8**: 943.
- Clark J, Crean S, Reynolds MW (2008). Topical bovine thrombin and adverse events: A review of the literature. *Current Medical Research and Opinion* **24**: 2071–2087.
- Chen BJ, Byrne FL, Takenaka K, Modesitt SC, Olzomer EM et al. (2018). Analysis of the circular RNA transcriptome in endometrial cancer. *Oncotarget* **9**: 5786–5796.
- Choi SK, Park JK, Kim JH, Lee KM, Kim E et al. (2016). Integrin-binding elastin-like polypeptide as an *in situ* gelling delivery matrix enhances the therapeutic efficacy of adipose stem cells in healing full-thickness cutaneous wounds. *Journal of Controlled Release* **237**: 89–100.
- Dreifke MB, Jayasuriya AA, Jayasuriya AC (2015). Current wound healing procedures and potential care. *Materials Science and Engineering C* **48**: 651–662.
- Fehse B, Chukhlovin A, Kuhlcke K, Marinetz O, Vorwig O et al. (2001). Real-time quantitative Y chromosome-specific PCR (QYCS-PCR) for monitoring hematopoietic chimerism after sex-mismatched allogeneic stem cell transplantation. *Journal of Hematotherapy & Stem Cell Research* **10**: 419–425.
- Gelmini S, Tricarico C, Vona G, Livi L, Melina AD et al. (2001). Real-Time quantitative reverse transcriptase-polymerase chain reaction (RT-PCR) for the measurement of prostate-specific antigen mRNA in the peripheral blood of patients with prostate carcinoma using the taqman detection system. *Clinical Chemistry and Laboratory Medicine* **39**: 385–391.
- Gristina AG (1987). Biomaterial-centered infection: microbial adhesion vs. tissue integration. *Science* **237**: 1588–1595.
- Guyen MN, Altuncu MS, Bal T, Oran DC, Gulyuz U et al. (2018). Bisphosphonic acid-functionalized cross-linkers to tailor hydrogel properties for biomedical applications. *ACS Omega* **3**: 8638–8647.
- Hajimiri M, Shahverdi S, Esfandiari MA, Larijani B, Atyabi F et al. (2016). Preparation of hydrogel embedded polymer-growth factor conjugated nanoparticles as a diabetic wound dressing. *Drug Development and Industrial Pharmacy* **42**: 707–719.
- Han B, Chao J, Yao H (2018). Circular RNA and its mechanisms in disease: From the bench to the clinic. *Pharmacology & Therapeutics* **187**: 31–44.
- Han B, Woodell-May J, Ponticciello M, Yang Z, Nimni M (2009). The effect of thrombin activation of platelet-rich plasma on demineralized bone matrix osteoinductivity. *Journal of Bone & Joint Surgery* **91**: 1459–1470.
- Hashemi SS, Mahmoodi M, Rafati AR, Manafi F, Mehrabani D (2017). The role of human adult peripheral and umbilical

- cord blood platelet-rich plasma on proliferation and migration of human skin fibroblasts. *World Journal of Plastic Surgery* **6**: 198–205.
- Jeck WR, Sharpless NE (2014). Detecting and characterizing circular RNAs. *Nature Biotechnology* **32**: 453–461.
- Jessen KR, Mirsky R (2016). The repair Schwann cell and its function in regenerating nerves. *Journal of Physiology* **594**: 3521–3531.
- Jo CH, Lee SY, Yoon KS, Oh S, Shin S (2020). Allogeneic platelet-rich plasma vs. corticosteroid injection for the treatment of rotator cuff disease: A randomized controlled trial. *Journal of Bone & Joint Surgery* **102**: 2129–2137.
- Kim MH, Wu WH, Choi JH, Kim J, Jun JH et al. (2017). Galectin-1 from conditioned medium of three-dimensional culture of adipose-derived stem cells accelerates migration and proliferation of human keratinocytes and fibroblasts. *Wound Repair and Regeneration* **26**: S9–S18.
- La WG, Yang HS (2015). Heparin-conjugated poly(lactic-co-glycolic acid) nanospheres enhance large-wound healing by delivering growth factors in platelet-rich plasma. *Artificial Organs* **39**: 388–394.
- Lauffer M, Ashkenazi C, Katz D, Wolman M (1974). Orientation of collagen in wound healing. *British Journal of Experimental Pathology* **55**: 233–236.
- Luippold G, Klein T, Mark M, Grempler R (2012). Empagliflozin, a novel potent and selective SGLT-2 inhibitor, improves glycaemic control alone and in combination with insulin in streptozotocin-induced diabetic rats, a model of type 1 diabetes mellitus. *Diabetes, Obesity and Metabolism* **14**: 601–607.
- Max N, Wolf K, Spike B, Thiel E, Keilholz U (2001). Nested quantitative real time PCR for detection of occult tumor cells. In: Reinhold U, Tilgen W (eds.), *Minimal Residual Disease in Melanoma. Recent Results in Cancer Research*. Berlin, Heidelberg: Springer.
- Mcardle C, Lagan KM, Mcdowell DA (2014). The pH of wound fluid in diabetic foot ulcers—the way forward in detecting clinical infection? *Current Diabetes Reviews* **10**: 177–181.
- Michalczyk ER, Chen L, Maia MB, Dipietro LA (2020). A role for low-density lipoprotein receptor-related protein 6 in blood vessel regression in wound healing. *Advances in Wound Care* **9**: 1–8.
- Murphy MB, Blashki D, Buchanan RM, Yazdi IK, Ferrari M et al. (2012). Adult and umbilical cord blood-derived platelet-rich plasma for mesenchymal stem cell proliferation, chemotaxis, and cryo-preservation. *Biomaterials* **33**: 5308–5316.
- Nakanishi H, Kodera Y, Yamamura Y, Tatematsu M (2001). Rapid quantitative detection of free cancer cells in the peritoneal cavity of gastric cancer patients with real-time RT-PCR, and its prognostic significance. *Gan To Kagaku Ryoho* **28**: 784–788.
- Natarajan S, Williamson D, Stiltz AJ, Harding K (2000). Advances in wound care and healing technology. *American Journal of Clinical Dermatology* **1**: 269–275.
- Petersen A, Princ A, Korus G, Ellinghaus A, Leemhuis H et al. (2018). A biomaterial with a channel-like pore architecture induces endochondral healing of bone defects. *Nature Communications* **9**: 4430.
- Ponsubha S, Jaiswal AK (2020). Effect of interpolymer complex formation between chondroitin sulfate and chitosan-gelatin hydrogel on physico-chemical and rheological properties. *Carbohydrate Polymers* **238**: 116179.
- Previtali SC, Nodari A, Taveggia C, Pardini C, Dina G et al. (2003). Expression of laminin receptors in Schwann cell differentiation: Evidence for distinct roles. *Journal of Neuroscience* **23**: 5520–5530.
- Qiu M, Chen D, Shen C, Shen J, Zhao H, He Y (2016). Platelet-rich plasma-loaded poly(D,L-lactide)-poly(ethylene glycol)-poly(D,L-lactide) hydrogel dressing promotes full-thickness skin wound healing in a rodent model. *International Journal of Molecular Sciences* **17**: 1001.
- Rebulla P, Pupella S, Santodirocco M, Greppi N, Villanova I et al. (2016). Multicentre standardisation of a clinical grade procedure for the preparation of allogeneic platelet concentrates from umbilical cord blood. *Blood Transfusion* **14**: 73–79.
- Rousselle P, Montmasson M, Garnier C (2019). Extracellular matrix contribution to skin wound re-epithelialization. *Matrix Biology* **75-76**: 12–26.
- Saidian M, Lakey JRT, Ponticorvo A, Rowland R, Baldado M et al. (2019). Characterisation of impaired wound healing in a preclinical model of induced diabetes using wide-field imaging and conventional immunohistochemistry assays. *International Wound Journal* **16**: 144–152.
- Shi K, Wang YL, Qu Y, Liao JF, Chu BY et al. (2016). Synthesis, characterization, and application of reversible PDLLA-PEG-PDLLA copolymer thermogels *in vitro* and *in vivo*. *Scientific Reports* **6**: 19077.
- Steed DL, Attinger C, Colaizzi T, Crossland M, Franz M et al. (2006). Guidelines for the treatment of diabetic ulcers. *Wound Repair and Regeneration* **14**: 680–692.
- Thomson SE, Mclennan SV, Hennessy A, Boughton P, Bonner J et al. (2010). A novel primate model of delayed wound healing in diabetes: dysregulation of connective tissue growth factor. *Diabetologia* **53**: 572–583.
- Van Elden LJ, Nijhuis M, Schipper P, Schuurman R, van Loon AM (2001). Simultaneous detection of influenza viruses A and B using real-time quantitative PCR. *Journal of Clinical Microbiology* **39**: 196–200.
- Wang Y, Hung C, Koh D, Cheong D, Hooi SC (2001). Differential expression of Hox A5 in human colon cancer cell differentiation: A quantitative study using real-time RT-PCR. *International Journal of Oncology* **18**: 617–622.
- Xue S, Wu Y, Guo M, Xia Y, Liu D et al. (2019). Self-healable poly(acrylic acid-co-maleic acid)/glycerol/boron nitride nanosheet composite hydrogels at low temperature with enhanced mechanical properties and water retention. *Soft Matter* **15**: 3680–3688.
- Yang Y, Zhang J, Liu Z, Lin Q, Liu X et al. (2016). Tissue-integratable and biocompatible photogelation by the imine crosslinking reaction. *Advanced Materials* **28**: 2724–2730.
- Zhu Y, Hoshi R, Chen S, Yi J, Duan C et al. (2016). Sustained release of stromal cell derived factor-1 from an antioxidant thermoresponsive hydrogel enhances dermal wound healing in diabetes. *Journal of Controlled Release* **238**: 114–122.